Pathways for Formation and Chlorination of Carbazole, Phenoxazine and Phenazine

Mohammednoor Altarawneh*†, Bogdan Z. Dlugogorski

School of Engineering and Information Technology

Murdoch University, Perth, WA 6150, Australia

*Corresponding Author:

Phone: (+61) 8 9360-7507

Fax: (+61) 8 9360 6346

E-mail: M.Altarawneh@Murdoch.edu.au

† On leave from Chemical Engineering Department, Al-Hussein Bin Talal University, Ma'an, Jordan

Abstract

This contribution presents pathways for the formation of the three nitrogenated dioxin-like species, carbazole, phenoxazine and phenazine via unimolecular rearrangements of diphenylamine (**DPA**) and its nitro substituents (**NDPA**). The latter represent major structural entities appearing in formulations of explosives and propellants. Intramolecular H transfer from the amine group to one of the two O atoms in the nitro group denotes the most accessible route in the unimolecular decomposition of **NDPA**. Further unimolecular rearrangements afford phenazine and carbazole. A loss of an ortho substituent from **DPA**, followed by addition of an oxygen molecule, prompts the formation of carbazole and phenoxazine in a facile mechanism. The consistency between trends in Fukui-based electrophilic indices and the experimental profiles of chlorinated carbazole, phenoxazine and phenazine suggests the formation of these species by electrophilic substitution.

Introduction

Nitrogenated analogues of polychlorinated dibenzo-*p*-dioxins and polychlorinated dibenzofurans (aka PCDD/Fs or dioxins) represent a group of novel persistent organic pollutants (POPs). This group contains diphenylamine (DPA), carbazole, phenoxazine and phenazine:

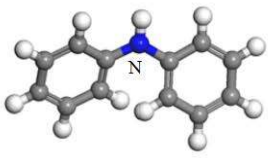

DPA

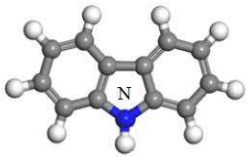

Carbazole

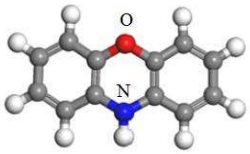

Phenoxazine

Phenazine

Due to their dioxin-like ecotoxicological features,[1,2] these compounds attract mounting environmental and health concerns. The current consensus of opinion points to the natural formation of these compounds.[3-5] However, carbazole, in particular, occurs as a product in incineration of industrial wastes[6] and combustion of biomass[7] suggesting that these species could also arise from thermal processes in pathways equivalent to those forming the notorious PCDD/Fs congeners.[8]

A study by Cropek at al.[9] on pyrolysis of an army-type propellant indicated that, disposal of hazardous wastes from armaments industry via incineration results in the formation of several nitrogen-containing hetrocyclic aromatics. By experimenting with 2-nitrodiphenylamine, (NDPA or 2-nitro-*N*-diphenylamine), a structural entity present in propellants:

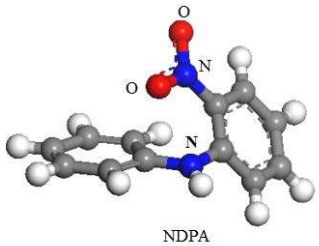

NDPA

Cropek at al.[9] found the major pyrolytic products to comprise phenazine and carbazole. Furthermore, the use of explosives in mining may represent a worst-case scenario for the emission of congeners of nitrogenated dioxin-like species. Nevertheless, literature on emission of nitrogen-containing compounds from mining-related activities[10] has been limited to formation of NO_X with no measurements of carbazole, phenoxazine and phenazine.

DPA and its derivatives are important intermediates in many industrial applications; most notably, in dyes, antioxidants and nitrocellulose-containing explosives and propellants.[11] Beside their formation as natural products,[12] the dispersive applications of **DPA** have contributed to their widespread presence in the environment.[13] The structural resemblance between **DPA** and the three other nitrogenated heterocyclic compounds suggests that, **DPA** acts as a building block for the formation of carbazole, phenoxazine and phenazine. Biodegradation of **DPA** constitutes a potent source of carbazole and phenazine in the environment.[11,14,15]

Literature does not explain mechanisms responsible for thermal conversion of **DPA** and its derivatives into the three nitrogenated heterocyclic compounds. If developed, such mechanisms would elucidate the contribution of an anthropogenic route to the global inventory of nitrogenated dioxin-like compounds. In this study, we utilise density functional theory (DFT) calculations to develop pathways for the formation of carbazole, phenoxazine and phenazine from **DPA** and its NO_2 substituted, **NDPA,** to shed light onto their chlorination patterns.

Theoretical Methodology

The Gaussian09 programme[16] facilitated all structural optimisations and energy calculations at the theoretical level of M062X/6-311+G(d,p). The M062X meta hybrid functional[17] was designed to afford satisfactory performance in general kinetic and thermochemical applications in organic systems. We have recently shown[18] that, refining M062X-obtained energies, via performing single point energy calculations on a bigger basis sets, changes final calculated reaction and activation enthalpies only marginally (i.e. within 0.50 kcal/mol). The search of transition structures often follows a broken summery approach. We carry out intrinsic reaction coordinate (IRC) calculations to link transition structures with their perspective reactants and products. The KisThelP[19] code provided estimates of kinetic parameters. A one-dimensional Eckart functional[20] accounted for the plausible contributions from quantum tunnelling effects. We fitted rate constants to modified Arrhenius parameters over the temperature range of 400 K – 1500 K. Table 1 enlists reaction rate constants for selected reactions. All discussed energetics refer to enthalpic values calculated at 298.15 K. The Dmol^3 code[21] served to estimate Hirshfeld[22] charge distributions and Fukui indices[23] of electrophilic attack ($f^{-1}(r)$) on a particular atom based on the BLYP[24] functional and the DND basis set. Calculation of global electophilicity factors (ω) relied on chemical potential (μ) and chemical hardness (η), according to a formula introduced by Parr et al.[25]:

$$\omega = \frac{\mu^2}{2\eta}$$

where μ and η are estimated from energies of the highest ($\varepsilon_{\mathrm{HOMO}}$) and lowest ($\varepsilon_{\mathrm{LOMO}}$) occupied molecular orbitals:

$$\mu = \frac{1}{2}(\varepsilon_{\mathrm{HOMO}} + \varepsilon_{\mathrm{LOMO}}) \qquad \eta = \frac{1}{2}(\varepsilon_{\mathrm{HOMO}} - \varepsilon_{\mathrm{LOMO}})$$

Values of electophilicity factors help to assess the tendency of an isomer to undergo electrophilic-like chlorination, including the type of congener produced, as function of prior chlorination.

Results and Discussion

Routes for formation of carbazole, phenoxazine and phenazine

Guided by the experimental results of Cropek et al.,[9] we first examined reaction pathways operating in the self-decomposition of the **NDPA** molecule. We illustrate that, the most accessible initial exit channels in the degradation of **NDPA** lead principally to the formation of carbazole and phenazine, in an agreement with the profile of experimentally detected products. Figure 1 displays reaction and activation enthalpies for all plausible unimolecular corridors.

Four of the investigated pathways comprise barrierless fissions of N-H and aromatic C-NO_2 bonds and breakage of one of the two ends of the –N(H)– bridge. Performing partial optimisation along reaction coordinates of these pathways confirms lack of genuine transition structures for these bond breakage reactions. The curves of minimum energy points (MEPs) for these four reactions increase monotonically, without passing through a saddle point.

126 Generally, simple bond fissions in stable molecules occur without encountering transition
127 structures (i.e. $C_2H_6 \rightarrow 2CH_3$).
128
129 Rupture of one of the two –N(H)– linkages takes place via endothermic reactions of 88.7
130 kcal/mol and 93.8 kcal/mol. Scission of the N-H bond is predicted to be endothermic by 86.1
131 kcal/mol. This value compares very well with the corresponding bond dissociation enthalpy
132 (BDH) in the aniline molecule, i.e. ~ 90.0 kcal/mol.[26] The C-NO_2 bond is the weakest in the
133 **NDPA** molecule with its BDH of 70.6 kcal/mol. This value concurs with the experimental
134 BDH associated with the loss of a nitro group from a nitrobenzene molecule of 72.1
135 kcal/mol.[26] Part of Figure 1 depicts a closed-shell ring-closure reaction leading to the
136 formation of a carbazole molecule. The transition structure TS1 tracks the attachment of the
137 carbon bearing the nitro group, to a carbon, *ortho* to the –N(H)- bridge, on the neighbouring
138 phenyl ring, with a simultaneous expulsion of the NO_2 moiety. Enthalpic barrier of this
139 reaction amounts to 65.0 kcal/mol and the reaction produces the M8 pre-carbazole
140 intermediate. The out-of-plane H atom departs the M8 radical via an activation enthalpy of
141 20.7 kcal/mol (TS2) yielding a carbazole molecule accompanied with a modest
142 endothermicity of 11.9 kcal.
143
144 The presence of a relatively weak N-H bond in the **NDPA** molecule opens up an
145 intramolecular hydrogen transfer from the NH moiety toward one of the two oxygen atoms in
146 the NO_2 group. This reaction occurs via a reaction barrier of 36.4 kcal/mol and takes place
147 via TS3. Produced from this channel is the M7 intermediate, residing 30.6 kcal/mol above
148 the parent **NDPA** molecule. In the next step, barrierless fission of the N-OH bond in the M7
149 molecule affords the M9 radical. This barrierless loss of OH is associated with an enthalpic
150 change of 40.6 kcal.

Two channels compete for the fate of M9. The first pathway characterises a C-C bridging reaction with the simultaneous departure of NO moiety. This corridor necessitates a sizable activation enthalpy of 39.1 kcal/mol (TS4) and results in the formation of the M11 intermediate. Transformation of the latter into a carbazole molecule occurs in a two-step process. The first step characterises 1,2-hydrogen transfer through TS8 (25.5 kcal/mol) and results in the formation of the diradical M14. Formation of carbazole from M14 in the second step entails a considerable exothermicity of 58.7 kcal and takes place through a trivial activation enthalpy of 6.1 kcal/mol (TS9). In an alternate pathway, the nitrogen atom of the NO group in the M9 radical attacks a carbon atom, *ortho* to the –-N(H)- link, on the neighbouring phenyl ring. This ring-cyclisation reaction requires a rather low activation enthalpy at 11.5 kcal/mol (TS5) and produces the M10 intermediate. Finally, a phenazine molecule arises from the M10 intermediate through two intramolecular hydrogen transfer reactions (M10 → M12 and M12 → M13) and a unimolecular loss of a hydroxyl group (M13 → Phenazine + OH). The two hydrogen transfer reactions require modest activation enthalpies of 27.2 kcal/mol (TS6) and 25.8 kcal/mol (TS7). The loss of the OH moiety from the M13 intermediate occurs via TS11 through an activation enthalpy of 17.1 kcal/mol.

Inspection of the kinetic parameters in Table 1 reveals that intramolecular H transfer controls the unimolecular decomposition of the **NDPA** molecule at all temperatures. The kinetics of the initiation reaction (NPDA → M7) dominate all other plausible channels. This concurs with the experimental finding of phenazine being the most abundant product from pyrolysis of **NDPA**. Cyclisation of the M9 radical into the M10 intermediate prevails over the ring-closure reaction of M9 → M11 + NO.

176 We have recently presented comprehensive mechanisms for the oxidative transformation of
177 halogenated diphenyl ethers into polychlorinated dibenzo-*p*-dioxins and polychlorinated
178 dibenzofurans[27] and their brominated counterparts (PBDD/Fs).[28] Analogously, Figure 2
179 illustrates that initial oxidation of a **DPA** molecule leads to the formation of carbazole and
180 phenoxazine molecules in facile mechanisms. Central to the mechanisms of Figure 2 is the
181 formation of a peroxyl-type adduct at an *ortho* position (M16) followed by unimolecular
182 isomerisation of this adduct into a three-cyclic structure (M18). Subsequent steps include
183 bridging (M18 → M19), ring-closure (M19 → M21), and enolisation (M21 → M22)
184 reactions. A carbazole molecule arises from the direct *ortho* C – *ortho* C bridging (M15 →
185 M2). The profound importance of the mechanisms presented in Figure 2 is evident from the
186 low activation enthalpies reported for all steps (i.e. ≤ 30.0 kcal/mol). Kinetic parameters for
187 barrierless reactions, that are not included in Table 1, could readily be extracted from
188 analogous systems in the literature. For instance, reaction rate constants for the formation of
189 the peroxyl- (M16) and phenoxy- (M17) type adducts could be assigned similar values with
190 the correponding reactions in the phenylperoxy system.[29]
191
192 Along the same line of enquiry, aniline ($C_6H_5NH_2$) is a major product from
193 combustion/pyrolysis of various nitrogen-containing fuels.[30] Thus, we investigated the
194 possibility that aniline (and its derived anilino radical) acts as a potential precursor for the
195 formation of carbazole, phenazine and phenoxazine. By considering aniline and anilino
196 (C_6H_5NH) as building blocks, we followed well-established mechanisms for the gas phase
197 formation of PCDD/Fs and PBDD/Fs from chlorophenols[8] and bromophenols, respectively.
198 While we were able to locate stable analogous nitrogenated intermediates, and despite of our
199 best efforts, we were unsuccessful in locating necessary transition structures along relevant
200 reaction pathways. The role of aniline and other nitrogen aromatics (i.e. nitrobenzene) in the

formation of the nitrogenated analogous of dioxins (carbazole, phenoxazine and phenazine) warrants further investigation.

Chlorination via electrophilic substitution

Having presented potential pathways for the formation of the three nitrogenated dioxin-like compounds, we are now in a position to elucidate some insight into their chlorination patterns. Data on environmental occurrence and concentration of halogenated phenoxazine and phenazine are rather scarce. In contrast, halogenated substituents of carbazole have been readily measured in sediments, soils and water bodies.[31-36] It might be worthwhile mentioning in this context that, atomic numbering in the carbazole molecule is different from that of dibenzofuran:

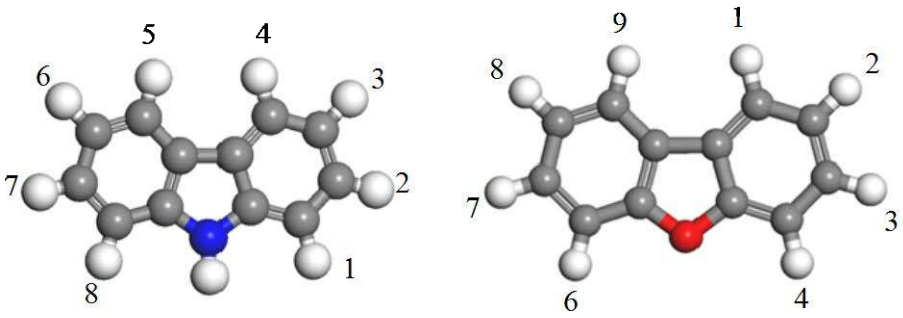

Carbazole Dibenzofuran

Carbazole congeners with halogen substitutions in the 1, 3, 6 and 8 positions dominate the isomer distribution in each homologue group. For example, 1,8-dibromo-3,6-dichlorocarbazole and 1,3,6,8-tetrabromocarbazole represent the only halogenated carbazole isomers that appear in rural sediments, whose concentration reached measurable levels.[31] Enzyme-induced chlorination of carbazole was found to afford predominantly two congeners, 3-monochlorocarbazole and 3,6-dichlorocarbazole.[35,36]

In case of other halogenated aromatics, thermodynamic stability correlates well with the relative abundance of chlorinated congeners.[37] Bearing in mind the significant random behaviour of gas phase chlorination,[8] thermodynamic stability does not provide a conclusive fingerprint pertinent to the operating chlorination mechanism. For example, we have shown that H abstraction from the four distinctive positions in dibenzofuran by H[38] and OH[39] radicals incur very similar activation barriers. Thus, there is a need to develop a more robust descriptor to account for the observed halogenation patterns. Among the numerous suggested chlorination mechanisms of POPs (i.e. by gaseous Cl radicals, ligand Cl transfer, Deacon reactions, .., etc),[8] chlorination by electrophilic substitution remains the most plausible mechanism,[40] especially in heterogeneous pathways. In this regard, Mumbo et al.[35] explained the regioselectivity in observed halogenation by means of reaction enthalpies for the formation of σ-complexes that arise in the first step of the electrophilic substitution:

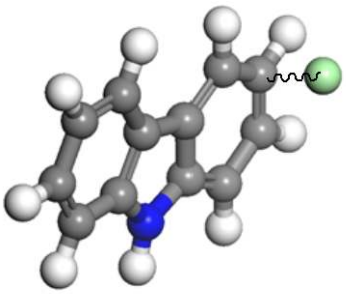

σ complex formed during the electrophilic chlorination of 3-chlorocarbazole

Herein, we explain the experimentally observed chlorination sequence of carbazole based on Fukui indices of electrophilic attack, $f^{-1}(r)$. Fukui analysis provides a general approach to investigate the reactivity of a compound to involve itself in a chemical reaction.[41,42] Values of $f^{-1}(r)$ originate from charge density and relevant properties of frontier molecular orbitals.

As an illustrative example, Figures 3 and 4 portray charge density distributed on a carbazole molecule and its HOMO/LUMO orbitals, respectively. The larger the value of $f^{-1}(r)$ on a certain atom, the more probability that this atom be accessible to electrophilic chlorination. Figures 5 and 6 show estimated $f^{-1}(r)$ values for carbazole chlorination and bromination patterns, respectively. It is evident from Figures 5 and 6 that chlorination and bromination of carbazole follows the same pattern. The tendency of carbazole to undergo halogenation via electrophilic substitution follows the sequence of $3 \rightarrow 6 \rightarrow 1 \rightarrow 8 \rightarrow 4 \rightarrow 5 \rightarrow 2$. Our predicted chlorination pattern matches the experimentally established dominance of 3-chloro-, 3,6-dichloro- and 1,3,6,8-tetrachlorocarbazole, each in its corresponding homologue group.

The consistency between trends in $f^{-1}(r)$ values and the experimental profiles of the most prominent congeners supports the occurrence of chlorination through electrophilic substitution. We could not deduce unified trends regarding the dependence of ω factors on the degree of chlorination (Figure 5). However, it is interesting to observe that, the 1,3,6,-trichlorocarbazole isomer holds the highest ω value. This in turn indicates that, the formation of this congener is associated with a profound tendency to undergo further chlorination into the 1,3,6,8-tetrachlorocarbazole congener via electrophilic substitution; i.e., the halogenation pattern which has been observed experimentally for carbazole. Figure S1 in the Supporting Information depicts chlorination patterns for phenoxazine and phenazine. Chlorination patterns of phenoxazine and phenazine are predicted to follow $3 \rightarrow 8 \rightarrow 7 \rightarrow 2 \rightarrow 4 \rightarrow 6$ and $1 \rightarrow 4 \rightarrow 2 \rightarrow 8 \rightarrow 6 \rightarrow 9$ sequences, in these respective orders.

In order to shed further light on a the occurrence of electrophilic substitutions as plausible dominant halogenation mechanism for POPs in general, we calculate in Table 2 $f^{-1}(r)$ values for chlorination and bromination sequences of PCDD/Fs. Chlorination pattern in Table 2

matches the corresponding homologue profile of PCDD/Fs formed by catalytic couplings of phenols over a $CuCl_2$ surface.[43]

To the best of our knowledge, the present contribution comprises the first attempt to link the halogenation pattern of a POP with the Fukui electrophilic indices. It will be helpful to construct Fukui-based halogenation patterns for other POPs and contrast them with experimentally measured signatures. This approach will afford reaching a generalised conclusion of whether the electrophilic substitution constitutes the dominant chlorination mechanism of POPs.

Conflict of Interest: The authors declare that they have no conflict of interest.

Acknowledgement

This study has been supported by a grant of computing time from the National Computational Infrastructure (NCI), Australia and the pawsey supercomputing facilities at Perth as well as funds from the Australian Research Council (ARC).

Supporting Information Available

Figure S1, Cartesian coordinates, total energies and vibrational frequencies for all structures. This material is available free of charge via the Internet at http://pubs.acs.org.

References

(1) Fink, J. K. In *High Performance Polymers (Second Edition)*; Fink, J. K., Ed.; William Andrew Publishing: 2014, p 42.

(2) Pohjanvirta, R.; Korkalainen, M.; McGuire, J.; Simanainen, U.; Juvonen, R.; Tuomisto, J. T.; Unkila, M.; Viluksela, M.; Bergman, J.; Poellinger, L.; Tuomisto, J. Comparison of Acute Toxicities of Indolo[3,2-B]Carbazole (Icz) and 2,3,7,8-Tetrachlorodibenzo-*p*-dioxin (TCDD) in TCDD-Sensitive Rats, *Food Chem Toxicol* **2002**, *40*, 1023.

(3) Thuy, T. T.; Lam, T. H.; Thanh Huong, N. T.; Hong Nhung, L. T.; Ninh, P. T.; Hoang Anh, N. T.; Phuong Thao, T. T.; Van Sung, T. Natural Phenoxazine Alkaloids from Peristrophe Bivalvis (L.) Merr, *Biochem Sys Ecol* **2012**, *44*, 205.

(4) Krishna C. M; Chattopadhya, S. K. *Heterocycles in Natural Product Synthesis*; Wiely, 2011.

(5) Arbiser, J. L.; Govindarajan, B.; Battle, T. E.; Lynch, R.; Frank, D. A.; Ushio-Fukai, M.; Perry, B. N.; Stern, D. F.; Bowden, G. T.; Liu, A.; Klein, E.; Kolodziejski, P. J.; Eissa, N. T.; Hossain, C. F.; Nagle, D. G. Carbazole Is a Naturally Occurring Inhibitor of Angiogenesis and Inflammation Isolated from Antipsoriatic Coal Tar, *J Invest Dermatol* **2006**, *126*, 1396.

(6) Ishikawa, S.; Sakazaki, Y.; Eguchi, Y.; Suetomi, R.; Nakamura, E. Identification of Chemical Substances in Industrial Wastes and Their Pyrolytic Decomposition Products, *Chemosphere* **2005**, *59*, 1343.

(7) Glarborg, P.; Jensen, A. D.; Johnsson, J. E. Fuel Nitrogen Conversion in Solid Fuel Fired Systems, *Prog. Energy Combust. Sci* **2003**, *29*, 89.

(8) Altarawneh, M.; Dlugogorski, B. Z.; Kennedy, E. M.; Mackie, J. C. Mechanisms for Formation, Chlorination, Dechlorination and Destruction of Polychlorinated Dibenzo-P-Dioxins and Dibenzofurans (Pcdd/Fs), *Prog. Energy Combust. Sci* **2009**, *35*, 245.

(9) Cropek, D. M.; Kemme, P. A.; Day, J. M.; Cochran, J. Use of Pyrolysis Gc/Ms for Predicting Emission Byproducts from the Incineration of Double-Base Propellant, *Environ. Sci. Technol.* **2002**, *36*, 4346.

(10) Jain, P.; Powell, J. T.; Smith, J. L.; Townsend, T. G.; Tolaymat, T. Life-Cycle Inventory and Impact Evaluation of Mining Municipal Solid Waste Landfills, *Environ. Sci. Technol.* **2014**, *48*, 2920.

(11) Drzyzga, O. Diphenylamine and Derivatives in the Environment: A Review, *Chemosphere* **2003**, *53*, 809.

(12) Karawya, M. S.; Wahab, S. M. A.; El-Olemy, M. M.; Farrag, N. M. Diphenylamine, an Antihyperglycemic Agent from Onion and Tea, *J. Nat. Prod.* **1984**, *47*, 775.

(13) Johnson, G. D.; Geronimo, J.; Hughes, D. L. Diphenylamine Residues in Apples (Malus Domestica Borkh.), Cider, and Pomace Following Commercial Controlled Atmosphere Storage, *J. Agr. Food Chem.* **1997**, *45*, 976.

(14) Shin K, A.; Spain J, C. Pathway and Evolutionary Implications of Diphenylamine Biodegradation by Burkholderia Sp. Strain Js667, *Appl. Environ. Microbiol.* **2009 75(9):**, *75*, 2694.

(15) Khang, H. Y.; Kukor, J. J.; Oh, K. H. Physiological and Phylogenetic Analysis of Burkholderia Sp. Hy1 Capable of Aniline Degradation, *World J Microb Biot* **2000**, *10*, 643.

(16) Frisch et al, M. J.; Gaussian 09. A.1 ed.; Gaussian, Inc: Wallingford CT, 2009.

(17) Zhao, Y.; Schultz, N. E.; Truhlar, D. G. Design of Density Functionals by Combining the Method of Constraint Satisfaction with Parametrization for Thermochemistry, Thermochemical Kinetics, and Noncovalent Interactions, *J. Chem. Theor. Comput.* **2006**, *2*, 364.

(18) Altarawneh, M.; Dlugogorski, B. Z. Formation of Dibenzofuran, Dibenozo-*p*-Dioxin and Their Hydroxylated Derivatives from Catechol, *Phys. Chem. Chem. Phys.* **2015**, ***17***, 18220.

(19) Canneaux, S.; Bohr, F.; Henon, E. Kisthelp: A Program to Predict Thermodynamic Properties and Rate Constants from Quantum Chemistry Results, *J. Comput. Chem.* **2014**, *35*, 82.

(20) Eckart, C. The Penetration of a Potential Barrier by Electrons, *Phys. Rev.* **1930**, *35*, 1303.

(21) Delley, B. From Molecules to Solids with the Dmol3 Approach, *J. Chem. Phys.* **2000**, *113*, 7756.

(22) Hirshfeld, F. L. Bonded-Atom Fragments for Describing Molecular Charge Densities, *Theoret. Chim. Acta* **1977**, *44*, 129.

(23) Fukui, K. Role of Frontier Orbitals in Chemical Reactions, *Science* **1982**, *218*, 747.

(24) Lee, C.; Yang, W.; Parr, R. G. Development of the Colle-Salvetti Correlation-Energy Formula into a Functional of the Electron Density, *Phys. Rev. B* **1988**, *37*, 785.

(25) Parr, R. G.; Szentpály, L. v.; Liu, S. Electrophilicity Index, *J. Am. Chem. Soc.* **1999**, *121*, 1922.

(26) Luo, R. Y. *Handbook of Bond Dissociation Energies in Organic*; CRC Press: Florida, Boca Raton, 1999.

(27) Altarawneh, M.; Dlugogorski, B. Z. Mechanisms of Transformation of Polychlorinated Diphenyl Ethers into Polychlorinated Dibenzo-*p*-dioxins and Dibenzofurans, *Chemosphere* **2014**, *114*, 129.

(28) Altarawneh, M.; Dlugogorski, B. Z. A Mechanistic and Kinetic Study on the Formation of PBDD/Fs from PBDEs, *Environ. Sci. Technol.* **2013**, *47*, 5118.

(29) Da Silva, G.; Bozzelli, J. W. Variational Analysis of the Phenyl + O_2 and Phenoxy + O Reactions, *J . Phys. Chem. A* **2008**, *112*, 3566.

(30) Lemieux, P. M.; Lutes, C. C.; Santoianni, D. A. Emissions of Organic Air Toxics from Open Burning: A Comprehensive Review, *Prog. Energy. Combust. Sci* **2004**, *30*, 1.

(31) Pena-Abaurrea, M.; Jobst, K. J.; Ruffolo, R.; Shen, L.; McCrindle, R.; Helm, P. A.; Reiner, E. J. Identification of Potential Novel Bioaccumulative and Persistent Chemicals in Sediments from Ontario (Canada) Using Scripting Approaches with Gc×Gc-Tof Ms Analysis, *Environ. Sci. Technol.* **2014**, *48*, 9591.

(32) Zhu, L.; Hites, R. A. Identification of Brominated Carbazoles in Sediment Cores from Lake Michigan, *Environ. Sci. Technol.* **2005**, *39*, 9446.

(33) Bonesi, S. M.; Erra-Balsells, R. On the Synthesis and Isolation of Chlorocarbazoles Obtained by Chlorination of Carbazoles, *J. Heterocyclic. Chem.* **1997**, *34*, 877.

(34) Kronimus, A.; Schwarzbauer, J.; Dsikowitzky, L.; Heim, S.; Littke, R. Anthropogenic Organic Contaminants in Sediments of the Lippe River, Germany, *Water Res.* **2004**, *38*, 3473.

(35) Mumbo, J.; Lenoir, D.; Henkelmann, B.; Schramm, K.-W. Enzymatic Synthesis of Bromo- and Chlorocarbazoles and Elucidation of Their Structures by Molecular Modeling, *Environ. Sci. Pollut. Res.* **2013**, *20*, 8996.

(36) Tröbs, L.; Henkelmann, B.; Lenoir, D.; Reischl, A.; Schramm, K.-W. Degradative Fate of 3-Chlorocarbazole and 3,6-Dichlorocarbazole in Soil, *Environ. Sci. Pollut. Res.* **2011**, *18*, 547.

(37) Wehrmeier, A.; Lenoir, D.; Schramm, K. W.; Zimmermann, R.; Hahn, K.; Henkelmann, B.; Kettrup, A. Patterns of Isomers of Chlorinated Dibenzo-*p*-dioxins as Tool for Elucidation of Thermal Formation Mechanisms, *Chemosphere* **1998**, *36*, 2775.

(38) Altarawneh, M.; Dlugogorski, B. Z.; Kennedy, E. M.; Mackie, J. C. Theoretical Study of Reaction Pathways of Dibenzofuran and Dibenzo-*p*-dioxin under Reducing Conditions, *J . Phys. Chem. A* **2007**, *111*, 7133.

(39) Altarawneh, M.; Kennedy, E. M.; Dlugogorski, B. Z.; Mackie, J. C. Computational Study of the Oxidation and Decomposition of Dibenzofuran under Atmospheric Conditions, *J. Phys. Chem .A.* **2008**, *112*, 6960.

(40) Munslow, W. D.; Sovocool, G. W.; Donnelly, J. R.; Mitchum, R. K. Electrophilic Bromination of Dibenzo-p-dioxin, *Chemosphere* **1987**, *16*, 1661.

(41) Szczepanik, D. W.; Mrozek, J. Nucleophilicity Index Based on Atomic Natural Orbitals, *J. Chem.* **2013**, *2013*, Article ID 684134.

(42) Thanikaivelan, P.; Padmanabhan, J.; Subramanian, V.; Ramasami, T. Chemical Reactivity and Selectivity Using Fukui Functions: Basis Set and Population Scheme Dependence in the Framework of B3LYP Theory, *Theor Chem Acc* **2002**, *107*, 326.

(43) Ryu, J.-Y.; Mulholland, J. A.; Takeuchi, M.; Kim, D.-H.; Hatanaka, T. $CuCl_2$-Catalyzed PCDD/F Formation and Congener Patterns from Phenols, *Chemosphere* **2005**, *61*, 1312.

Table 1: Arrhenius parameters (in temperature range 400 K – 1500 K). These parameters follow a modified Arrhenius rate expression; $k(T(\mathrm{K})) = AT^n \exp(-E_a / RT)$.

Reaction	A (s^{-1})	n	E_a (cal mol^{-1})
NDPA → M7	1.95×10^{12}	0.15	38 000
NDPA → M8 + NO_2	3.67×10^{13}	0.23	67 500
M8 → Carbazole + H	7.34×10^{13}	0.00	23 300
M9 → M11	8.65×10^{11}	0.00	36 700
M11 → M14	1.45×10^{12}	0.00	24 100
M14 → Carbazole + H	4.12×10^{13}	0.00	7 400
M9→ M10	5.35×10^{11}	1.12	12 000
M10→ M12	4.76×10^{11}	0.00	29 000
M12→ M13	8.31×10^{11}	0.00	24 100
M16 → M18	4.30×10^{11}	1.30	18 200
M15 → M2	6.67×10^{12}	0.00	10 000
M18 → M19	7.87×10^{-10}	0.65	32 500
M19 → M21	8.15×10^{12}	0.35	27 500
M17 → M20	1.13×10^{12}	0.73	23 800
M20 → Phenoxazine + OH	8.85×10^{12}	0.00	19 400
M20 → Phenoxazine + H	5.45×10^{13}	0.00	33 600

Table 2: Predicted chlorination pattern by electrophilic substitution of congeners of PCDD/F. Number in bold (red coloured) denote preferred chlorination sites. Close values of $f^{-1}(r)$ indicate multiple plausible chlorination sites.

	Congener	**1**	**2**	**3**	**4**	**6**	**7**	**8**	**9**
↓	**DD**	0.039	**0.063**	**0.063**	0.039	0.039	**0.063**	**0.063**	0.039
	2-MCDD	0.040	----	**0.058**	0.046	0.038	**0.059**	**0.061**	0.037
	2,8-DCDD	0.034	----	**0.056**	0.038	0.037	**0.054**	**----**	0.030
	2,3,8-TriCDD	0.029	----	**-----**	0.030	0.035	**0.053**	**----**	0.029
	2,3,7,8-TCDD	0.029	----	**-----**	0.029	0.029	**----**	**----**	0.029
↓	**DF**	0.054	0.064	**0.074**	0.056	0.056	**0.074**	0.064	0.054
	3-MCDF	0.048	0.051	----	0.046	0.046	**0.076**	0.054	0.049
	3,7-DCDF	**0.044**	**0.046**	----	0.040	0.040	**----**	**0.046**	**0.044**
	2,3,7-TriCDF	0.034	**----**	----	0.036	**0.040**	**----**	**0.042**	**0.043**
	2,3,7,8-TCDF	0.036	**----**	----	0.036	0.036	----	----	0.036

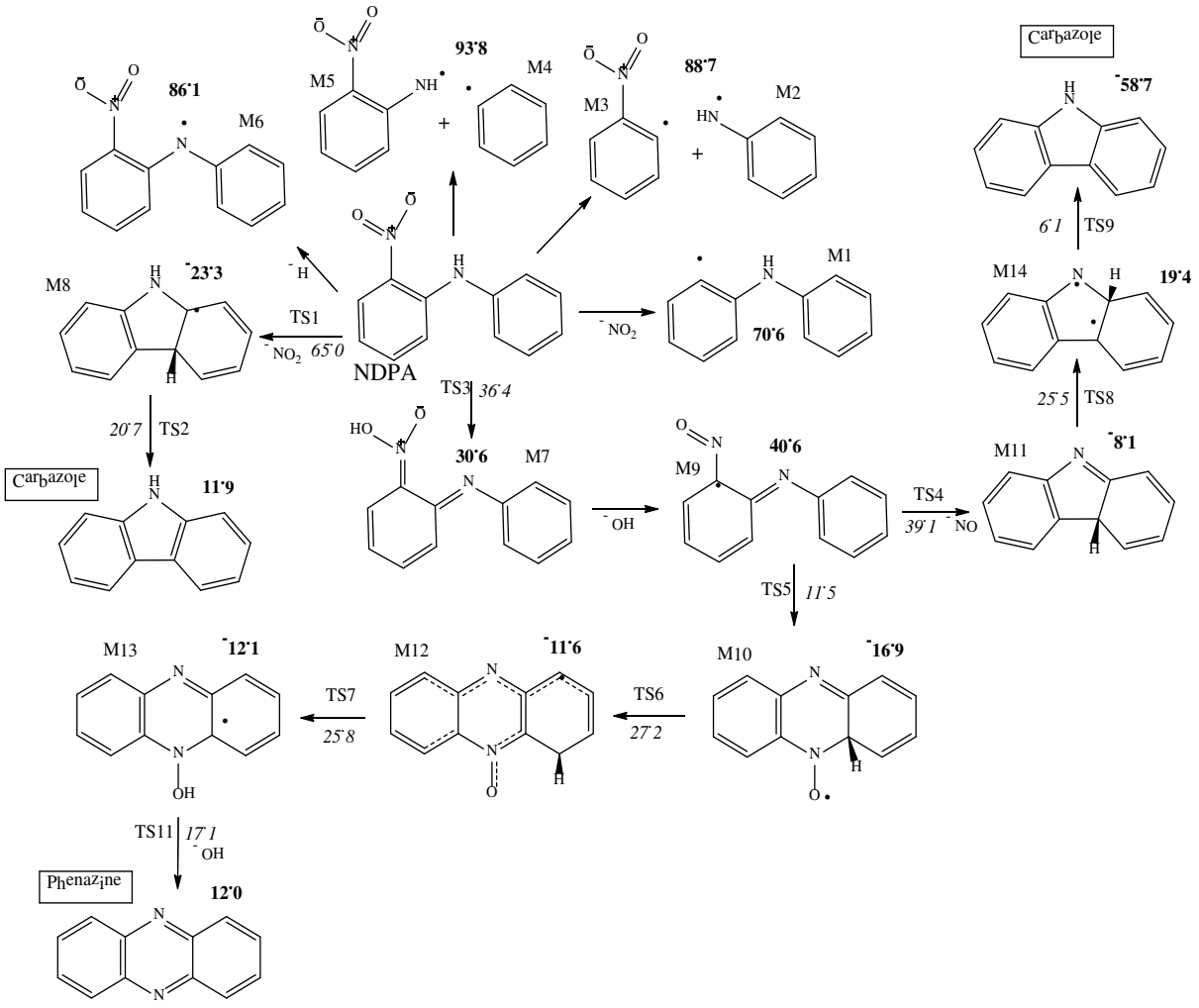

Figure 1. Pathways involved in the unimolecular decomposition of **NDPA** molecule. Values (with respect to reactant in each reaction) in bold and italic refer to reaction (in kcal) and activation (in kcal/mol) enthalpies, calculated at 298.15 K.

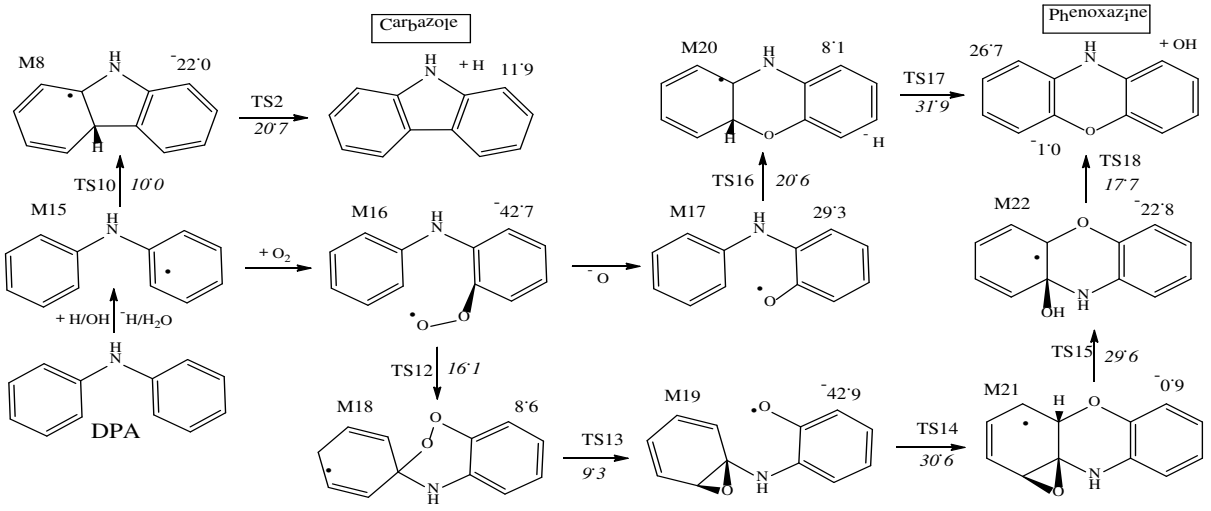

Figure 2. Pathways operating the self-degradation of a **DPA** molecule. Values (with respect to reactant in each reaction) in bold and italic refer to reaction (in kcal) and activation (in kcal/mol) enthalpies, calculated at 298.15 K.

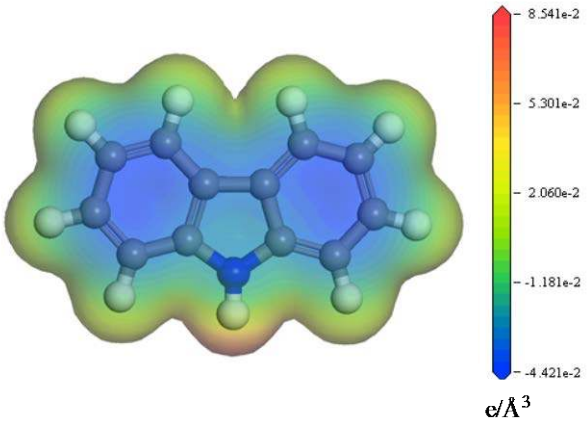

Figure 3. Electronic charge density on carbazole.

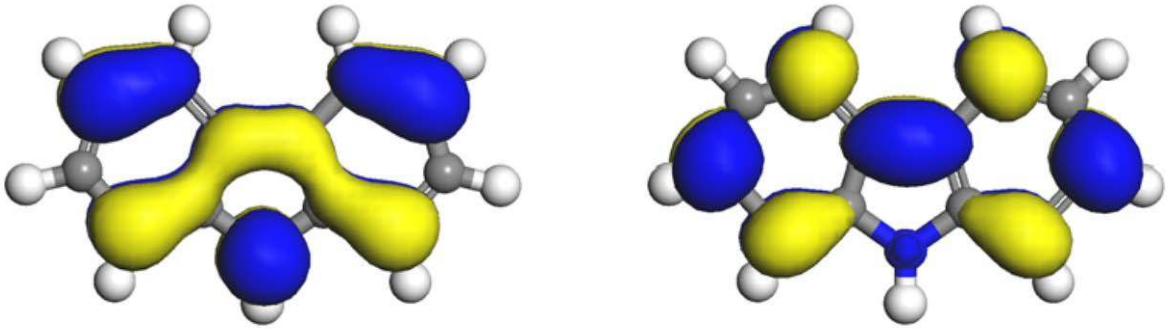

Figure 4. Frontier molecular orbitals of carbazole. The positive lobes of the orbital are light blue and the negative lobes are denoted by yellow colour.

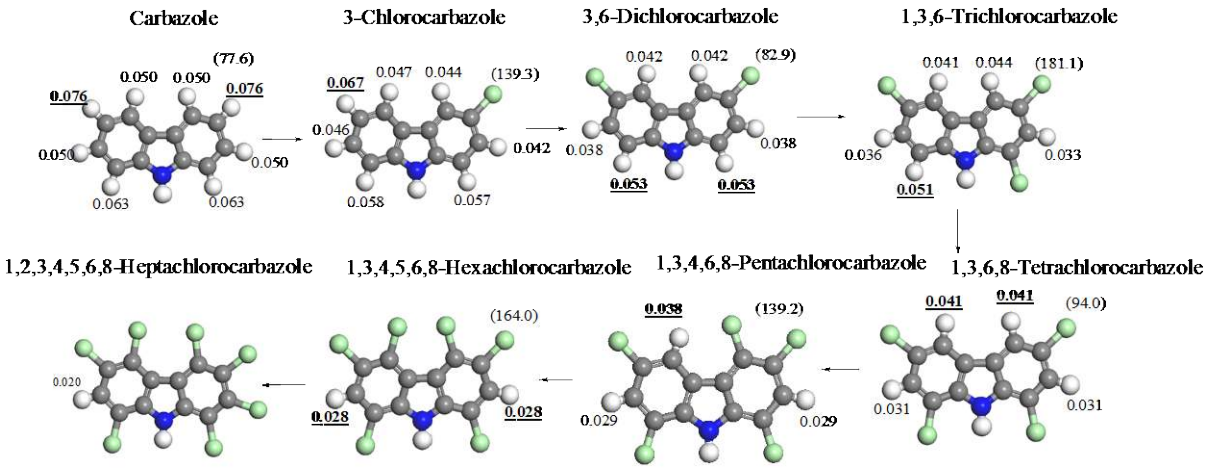

Figure 5. Chlorination sequence of carbazole predicted based on Fukui indices of electrophilic attack, $f^{-1}(r)$. Numbers in brackets denote global electrophilicity indices in kcal/mol.

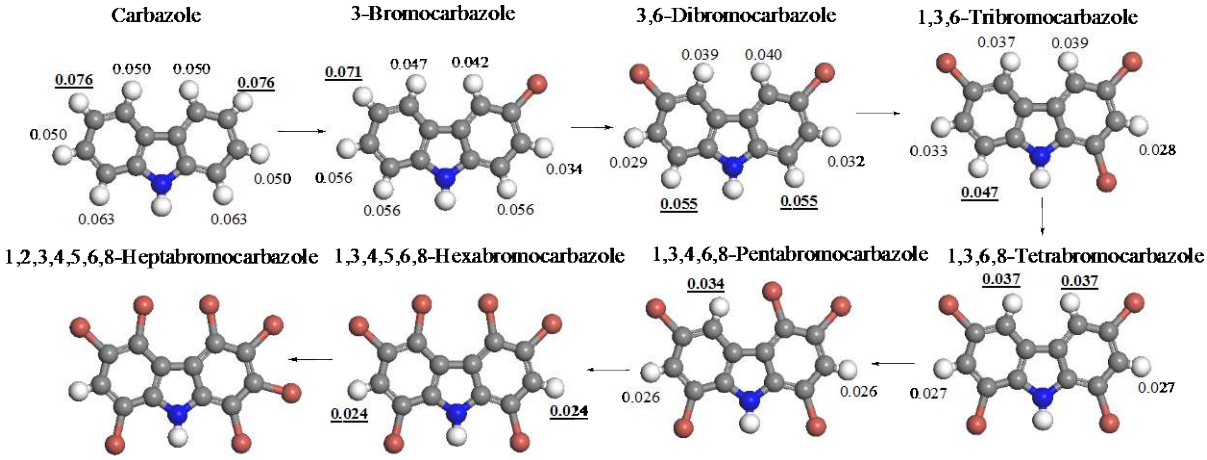

Figure 6. Bromination sequence of carbazole predicted based on Fukui indices of electrophilic attack, $f^{-1}(r)$.

TOC

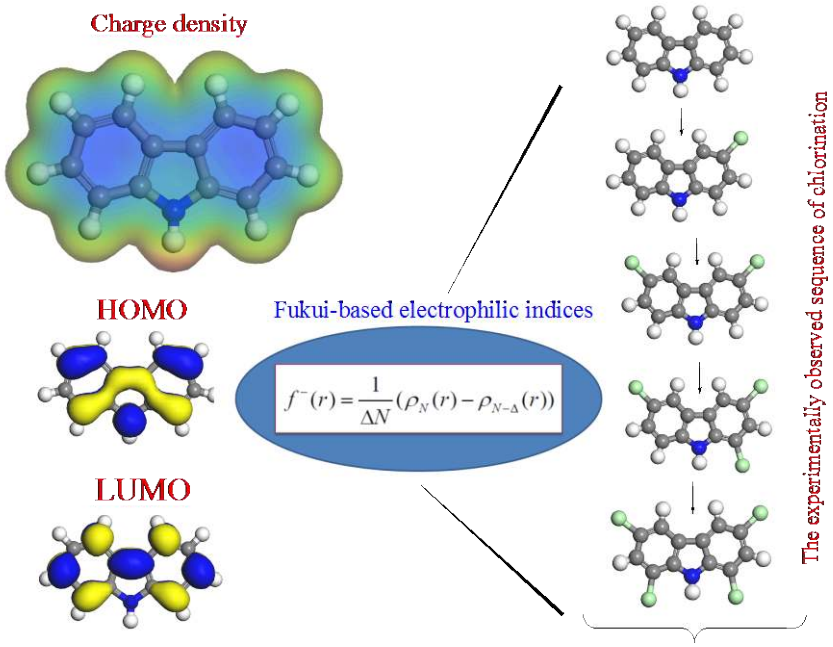
Charge density
HOMO
LUMO
Fukui-based electrophilic indices
$f^{-}(r)=\frac{1}{\Delta N}(\rho_{N}(r)-\rho_{N-\Delta}(r))$
The experimentally observed sequence of chlorination